Coupled Two-Electron/Halide Transfer Reactions of Ruthenoceniums and Osmoceniums

Timothy M. Shea, Samitha P. Deraniyagala,† Daniel B. Studebaker, and T. David Westmoreland*

Department of Chemistry, Wesleyan University, Middletown, Connecticut 06459

Received August 16, 1996[⊗]

Rate constants for the coupled two-electron/halide transfer self-exchange reactions of $[Cp_2MX]^+$ with Cp_2M (M = Ru, Os; X = Cl, Br) have been measured in CD_3CN at 298 K by 2D NMR spectroscopic techniques. Including data for the iodo complexes, the rates vary over 6 orders of magnitude depending on the metal and the halide, with the relative orderings I > Br > Cl and Ru > Os. The relative reactant state free energies for the ruthenium complexes have been determined from halide substitution equilibria and indicate that the reactant state energy ordering is Cl < Br < I. From these data and the free energies of activation for the self-exchange reactions, the relative transition state energies have been determined. A reaction coordinate and orbital correlation is proposed which rationalizes the observed data.

Introduction

The recognition that electron transfer reactions may proceed by inner-sphere or outer-sphere pathways[1,2] has provided a mechanistic framework for the rationalization of a tremendous amount of experimental redox data. Although progress has been made in defining the kinetics and thermodynamics of one-electron inner-sphere reactions,[1−4] considerably more attention has been directed toward understanding the details of one-electron outer-sphere reactions.[5]

Inner-sphere redox reactions that involve coupled multielectron/group transfers (often denoted "atom" transfers[6]) have been less well characterized. Of particular importance is the class of reactions which involve formal transfer of an oxygen atom, eq 1.[7,8] In eq 1, the formal oxidation state of X decreases by

$$X{=}O + Y \rightarrow X + O{=}Y \qquad (1)$$

2, while that of Y increases by 2. Such reactions are central to many redox processes in oxidoreductase enzymes, metal−oxo-based oxidations of organic molecules, and other catalytic redox systems. While several intermolecular multielectron/group transfer reactions have been characterized,[7−15] the critical parameters that govern the kinetics of such reactions have, however, not been fully explored. We have taken as a model system for oxygen atom transfer, and other coupled multielectron/group transfers, reaction 2, the self-exchange reaction of a halometallocenium with its corresponding metallocene.[9−11]

$$[Cp_2MX]^+ + Cp_2M \rightarrow Cp_2M + [Cp_2MX]^+ \qquad (2)$$

(M = Ru, Os; X = Cl, Br, I)

Reaction 2 corresponds to formal transfer of $[X]^+$, which is isoelectronic with oxygen atom. These systems are convenient for such studies since (1) most of their rates can be measured by dynamic NMR techniques and (2) synthetic variations of the metal, the transferred halogen, and the substituents on the cyclopentadienyl ring are accessible. The rates of several of these reactions have been previously characterized,[9−11] including some temperature, pressure, solvent, and counterion dependencies. From these previous studies, a number of key features of reaction 2 have been defined. (1) The reactions are inner-sphere electron transfers based on the volumes of activation.[10a,d] (2) The reactions are overall second order and are first order in both Cp_2M and $[Cp_2MX]^+$.[9,10b,c] (3) The rates of exchange vary over several orders of magnitude depending on the metal, halide, and cyclopentadienyl substitution.[9−11]

We have extended these previous studies by determining rates for several exchanges that were too slow to measure by conventional line-broadening techniques. Through the use of dynamic 2D NMR techniques, in particular, EXSY (exchange spectroscopy),[16] exchange rate constants of ≥ 0.01 s^{-1} are accessible. These results provide a more complete definition

† Permanent address: Department of Chemistry, University of Sri Jayawardenepura, Nugegoda, Sri Lanka.

⊗ Abstract published in *Advance ACS Abstracts,* December 1, 1996.

(1) (a) Taube, H. *Electron Transfer Reactions of Complex Ions in Solution,* Academic Press: New York, 1970. (b) Taube, H. *Angew. Chem., Int. Ed. Engl.* **1984,** *23,* 329−339.
(2) (a) Taube, H.; Myers, H.; Rich, R. L. *J. Am. Chem. Soc.* **1953**, *75,* 4118−4119. (b) Taube, H.; Myers, H. *J. Am. Chem. Soc.* **1954**, *76,* 2103−2111. (c) Taube, H.; King, E. L. *J. Am. Chem. Soc.* **1954**, *76,* 4053−4054.
(3) (a) Haim, A. *Acc. Chem. Res.* **1975**, *8,* 264−272. (b) Haim, A. *Prog. Inorg. Chem.* **1983**, *30,* 273−357.
(4) Endicott, J. F.; Kumar, K.; Ramasani, T.; Rotzinger, F. *Prog. Inorg. Chem.* **1983**, *30,* 141−187.
(5) Marcus, R. A.; Sutin, N. *Biochim. Biophys. Acta* **1985**, *811,* 265−322 and references therein.
(6) Taube, H. In *Mechanistic Aspects of Inorganic Reactions*; Rorabacher, D. B., Endicott, J. F., Eds.; ACS Symposium Series; American Chemical Society: Washington, DC, 1982; Vol. 198, pp 151−179.
(7) Holm, R. H. *Chem. Rev.* **1987**, *87,* 1401−1449 and references therein.
(8) Woo, L. K. *Chem. Rev.* **1993**, *93,* 1125−1136.
(9) Smith, T. P.; Iverson, D. J.; Droege, M. W.; Kwan, K. S.; Taube, H. *Inorg. Chem.* **1987**, *26,* 2882−2884.
(10) (a) Kirchner, K.; Dodgen, H. W.; Hunt, J. P.; Wherland, S. *Inorg. Chem.* **1989**, *28,* 604−605. (b) Kirchner, K.; Dodgen, H. W.; Hunt, J. P.; Wherland, S. *Inorg. Chem.* **1990**, *29,* 2381−2385. (c) Kirchner, K.; Han, L. F.; Dodgen, H. W.; Hunt, J. P.; Wherland, S. *Inorg. Chem.* **1990**, *29,* 4556−4559. (d) Anderson, K. A.; Kirchner, K.; Dodgen, H. W.; Hunt, J. P.; Wherland, S. *Inorg. Chem.* **1992**, *31,* 2605−2608.
(11) Watanabe, M.; Sano, H. *Chem. Lett.* **1991**, 555−558.
(12) (a) Woo, L. K.; Goll, J. G. *J. Am. Chem. Soc.* **1989**, *111,* 3755−3757. (b) Woo, L. K.; Czapla, D. J.; Goll, J. G. *Inorg. Chem.* **1990**, *29,* 3915−3916. (c) Woo, L. K.; Hays, J. A.; Goll, J. G. *Inorg. Chem.* **1990**, *29,* 3916−3917. (d) Woo, L. K.; Goll, J. G.; Czapla, D. J.; Hays, J. A. *J. Am. Chem. Soc.* **1991**, *113,* 8478−8484. (e) Bottomley, L. A.; Neely, F. L. *J. Am. Chem. Soc.* **1989**, *111,* 5955−5957.
(13) (a) Zhen, Y.; Feighery, W. G.; Lai, C.; Atwood, J. D. *J. Am. Chem. Soc.* **1989**, *111,* 7832−7837. (b) Zhen, Y.; Atwood, J. D. *Organometallics* **1991**, *10,* 2778−2780. (c) Wang, P.; Atwood, J. D. *J. Am. Chem. Soc.* **1992**, *114,* 6424−6427. (d) Wang, P.; Atwood, J. D. *Organometallics* **1993**, *12,* 4247−4249.
(14) Schwarz, C. L.; Bullock, R. M.; Creutz, C. *J. Am. Chem. Soc.* **1991**, *113,* 1225−1236.
(15) (a) Meyer, T. J. *J. Electrochem. Soc.* **1984**, *131,* 221C−228C. (b) Bakir, M; White, P. S.; Dovletoglov, A.; Meyer, T. J. *Inorg. Chem.* **1991**, *30,* 2835−2836.

S0020-1669(96)01000-2 CCC: $12.00

Table 1. Measured Self-Exchange Rates and Activation Parameters for $[Cp_2MX]^+/Cp_2M$ Self-Exchange Reactions at 298 K in CD_3CN

	k_{ex} (M^{-1} s^{-1}) (EXSY)	k_{ex} (M^{-1} s^{-1})[9,10] (line broadening)	$\Delta H^{\ddagger}$ (kJ/mol)	$T\Delta S^{\ddagger}$ (kJ/mol)	$\Delta G^{\ddagger}$ (kJ/mol)
$[Cp_2RuCl]^+/Cp_2Ru$	16.5 ± 0.1	*a*			(66)[b]
$[Cp_2RuBr]^+/Cp_2Ru$		1600	34.3 ± 0.4[c]	-19.6 ± 0.4[c]	53.9 ± 0.08[c]
	1950 ± 90		33 ± 3	-22.0 ± 0.2	54 ± 3
$[Cp_2RuI]^+/Cp_2Ru$	*d*	2.1×10^6	28.0 ± 0.8[c]	-11 ± 3[c]	39 ± 4[c]
$[Cp_2OsCl]^+/Cp_2Os$	1.64 ± 0.02	*a*			(72)[b]
$[Cp_2OsBr]^+/Cp_2Os$	23.8 ± 0.5	(3)[e]	47 ± 3	-18 ± 1	65 ± 4
$[Cp_2OsI]^+/Cp_2Os$	*d*	1.8×10^4	31.4 ± 0.4[c]	-17 ± 2[c]	48 ± 2[c]

[a] Too slow for line broadening. [b] Estimated from the rate at 298 K and the Eyring equation. [c] Reference 10d. [d] Coalesced at 298 K. [e] Estimated (ref 9).

of the range of rates exhibited by reaction 2. From determination of halide substitution equilibria for the haloruthenoceniums, the relative free energies of the transition states for the self-exchange reactions have been defined.

Experimental Section

Materials. Ruthenocene and osmocene were obtained from Strem Chemicals, Inc., and were sublimed prior to use. $[Cp_2MX]PF_6$ (M = Ru, Os; X = Cl, Br, I) were prepared by literature methods,[9] as were $(R_4N)X_2Y$ and $(R_4N)X_3$ (R = Me, Et, *n*-Bu; X, Y = Cl, Br, I).[17] CD_3CN for kinetic experiments was obtained from Cambridge Isotopes in sealed glass ampules and contained less than 1% water as determined by NMR. For other experiments, CD_3CN from Aldrich or Cambridge Isotopes was distilled over CaH_2 prior to use. Other materials were obtained commercially and used as received.

NMR Experiments. All NMR data were collected on a Varian Gemini 300 MHz spectrometer, and all chemical shifts reported are referenced to the solvent (CD_3CN; $\delta = 1.93$ ppm). Integrations of 1D and 2D data were performed using routines supplied by Varian. A Hewlett-Packard 8451A diode array UV−vis spectrophotometer was used for optical absorbance measurements.

To obtain kinetic data, appropriate amounts of $[Cp_2MX]PF_6$ and Cp_2M were weighed into an NMR tube and CD_3CN was added to give final concentrations near 5 mM. The relative concentrations of the two species were determined from a 1D NMR spectrum of the mixture. The absolute concentrations were obtained from optical absorbance data and the molar absorptivities of the $[Cp_2MX]^+$ species after the kinetic data were collected. The ^1H chemical shifts and molar absorptivities of the metallocenes and metalloceniums are summarized in the Supporting Information. A standard EXSY pulse sequence[16] was used to acquire the two-dimensional exchange data. For each experiment 256 1024W FIDs of eight scans each over a sweep width of 1600 Hz with a recycle delay of 0.1−4.0 s were collected in phase-sensitive mode. The integrated EXSY peak intensities were used to determine the exchange rate constant and variance as described previously[16,18,19] using the program MATW4, which performs mathematical functions on general real and complex matrices.[20] After each EXSY experiment the 1D spectrum was reacquired to ensure that no decomposition had occurred. A sample EXSY spectrum and a tabulation of the 2D integrals are given in the Supporting Information.

Halide Substitution Equilibria. Equilibrium constants for the halide substitution of haloruthenoceniums were obtained by mixing CD_3CN solutions of $[Cp_2RuX]PF_6$ with a substoichiometric amount (~0.1 molar ratio) of $(R_4N)XY_2$ or $(R_4N)Y_3$ at 298 K. The NMR spectrum of the mixture was monitored periodically until no further change was detected (6−12 h, depending on X and Y). At equilibrium, the NMR spectra showed the presence of $[Cp_2RuX]^+$, $[Cp_2RuY]^+$, and small amounts of Cp_2Ru. Integration of the peaks provided the $[Cp_2RuY]^+/[Cp_2RuX]^+$ ratios. The UV−vis spectra of the mixtures generally gave evidence for several mixed trihalides in addition to X_3^- and Y_3^-. The spectra were fit to a sum of the spectra of the individual species (typically $[Cp_2RuX]^+$, $[Cp_2RuY]^+$, Cp_2Ru, X_3^-, X_2Y^-, XY_2^-, and Y_3^-) by nonlinear least-squares techniques.[21] The fitting results for the mixtures are included in the Supporting Information. The resulting concentrations and standard deviations for the X_3^- and Y_3^- concentrations were then used for the estimation of the equilibrium constants for eq 3.

$$3[Cp_2RuX]^+ + Y_3^- \rightarrow 3[Cp_2RuY]^+ + X_3^- \qquad (3)$$

$$K_{([Cp_2RuX]^+,Y_3^-)} \cong \frac{[Cp_2RuY^+]^3[X_3^-]}{[Cp_2RuX^+]^3[Y_3^-]}$$

Results and Analysis

Self-Exchange Rates. In Table 1 are given the rates at 298 K for the self-exchange couples $[Cp_2MX]^+/Cp_2M$ (M = Ru, Os; X = Cl, Br, I). The EXSY approach extends the accessible NMR dynamic time scale to on the order of T_1 for the exchanging resonances. For both the oxidized and reduced metallocenes, values of T_1 in deoxygenated solutions are approximately 20 s.[22] Thus, the effective lower limit for the exchange rate accessible by EXSY in these systems is ~0.01 s^{-1}. The EXSY technique requires that two separate resonances be observed, and for the faster rates standard line-broadening techniques are more convenient. The data in Table 1 reflect both our EXSY results and the results of previous line-broadening studies.[9,10] The only couples that have exchange rates which are accessible by both dynamic NMR methods are the bromide transfer exchanges. For $[Cp_2RuBr]^+/Cp_2Ru$ the EXSY rate is similar to the previously measured value from line broadening. For the $[Cp_2OsBr]^+/Cp_2Os$ exchange, the rate is too slow for accurate determination using line broadening at temperatures below the solvent boiling point, but the value has been estimated to be 3 M^{-1} s^{-1}.[9] The EXSY experiment gives a value of 23.8 M^{-1} s^{-1}.

Table 1 also gives activation parameters for the self-exchange reactions in CD_3CN. The data in Table 1 represent a compilation of previously published results[10d] and values we have determined from temperature-dependent EXSY measurements (see Supporting Information). For $[Cp_2RuBr]^+/Cp_2Ru$, the activation parameters determined by line broadening compare well with those obtained by temperature-dependent EXSY. Each reaction has a large positive value of $\Delta H^{\ddagger}$ and a negative $\Delta S^{\ddagger}$ value. These parameters have been previously interpreted as

(16) (a) Jeener, J.; Meier, B. H.; Bachmann, P.; Ernst, R. R. *J. Chem. Phys.* **1979**, *71*, 4546−4553. (b) Macura, S.; Ernst, R. R. *Mol. Phys.* **1980**, *41*, 95−117. (c) Mendz, G. L; Robinson, G.; Kuchel, P. W. *J. Am. Chem. Soc.* **1986**, *108*, 169−173. (d) Abel, E. W.; Coston, T. P. J.; Orrell, K. G.; Sik, V.; Stephenson, D. *J. Magn. Reson.* **1986**, *70*, 34−53. (e) Dwyer, T. J.; Perrin, C. L. *Chem. Rev.* **1990**, *90*, 935−967.
(17) Chattaway, F. D.; Hoyle, G. *J. Chem. Soc.* **1923**, *123*, 654−662.
(18) Civitello, E. R.; Dragovich, P. S.; Karpishin, T. B.; Novick, S. G.; Bierach, G.; O'Connell, J. F.; Westmoreland, T. D. *Inorg. Chem.* **1993**, *32*, 237−241.
(19) Kuchel, P. W.; Bulliman, B. T.; Chapman, B. E.; Mendz, G. L. *J. Magn. Reson.* **1988**, *76*, 136−142.
(20) O'Connell, J. F. Unpublished.
(21) Program MRQMIN. Press, W. H.; Teukolsky, S. A.; Vetterling, W. T.; Flannery, B. P. *Numerical Recipes in Fortran*; 2nd ed.; Cambridge University Press: Cambridge, 1992; pp 678−683.
(22) Westmoreland, T. D. Unpublished results.

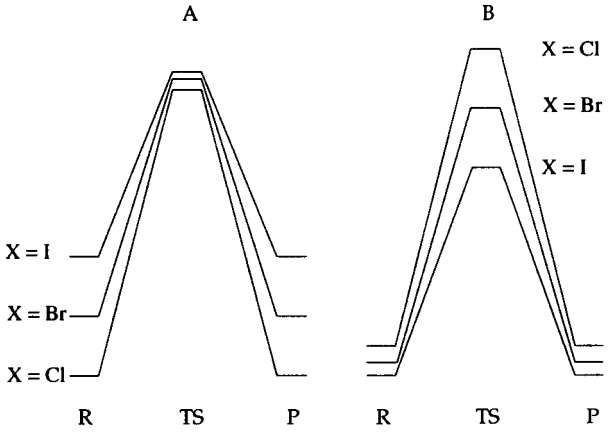

Figure 1. Limiting-case reaction coordinates for the $[Cp_2MX]^+/Cp_2M$ self-exchange reaction as a function of X (R = reactant state, TS = transition state, P = product state): (A) differential reactant state stabilization; (B) differential transition state stabilization.

Table 2. Equilibrium Constants and Free Energies for Halide Substitution Reactions 3 and 4 and Differential $\Delta G_f°$ for $[Cp_2RuX]^+$ in CD_3CN at 298 K

X	Y	$K_{([Cp_2RuX]^+,Y_3^-)}$	$\Delta G°_{([Cp_2RuX]^+,Y^-)}$ (kJ/mol)[a]	$\Delta\Delta G°_{(X,Y)}$ (kJ/mol)[b]
Br	I	18 ± 6	25 ± 5	63 ± 8
Cl	I	8 ± 10	49 ± 6	103 ± 8

[a] For reaction 4. [b] Defined in eq 7.

an indication of significant desolvation of the transition state relative to the reactant state.[10d]

Equilibrium constants for the halide substitution reaction in eq 3 $K_{([Cp_2RuX]^+,\ Y_3^-)}$ are included in Table 2 for X = Br or Cl, Y = I. In each case, the iodo complex is thermodynamically favored under the experimental conditions. These values do not, however, directly reflect the relative stabilities of the $[Cp_2RuX]^+$ cations since the formation of the trihalide products provides much of the driving force for these reactions (*vide infra*).

Discussion

The data in Table 1 extend the range and precision of measured self-exchange rates in the $[Cp_2MX]^+/Cp_2M$ series. As noted above, there is a very pronounced dependence on the identity of the transferred atom. As has been previously recognized, the halide dependence of the rates in these[9,10] and other[14] similar formal coupled two-electron/group transfers is generally several orders of magnitude larger than for formal one-electron transfers. The thermodynamic studies detailed above have allowed us to address the origin of the halide dependence of the rates.

There are two limiting cases for rationalizing the relative exchange rates with varying X, as illustrated in Figure 1. In case A, the reaction coordinate for each exchange proceeds through transition states that are nearly isoenergetic and the differences in the activation barriers arise primarily from the relative energies of the reactants. In this scenario, the rate differences might be interpreted as reflecting, for example, a large $M^{IV}-Cl$ bond strength and a much weaker $M^{IV}-I$ bond with a net decrease in the M−X bond order in the transition state. For case B, the differences in reactant state energies are small compared to the overall energetics along the reaction coordinate and the activation parameters are dominated by differences in transition state energies. Case B would suggest that the rate differences are related to a much larger affinity of the transition state for iodide than for chloride.

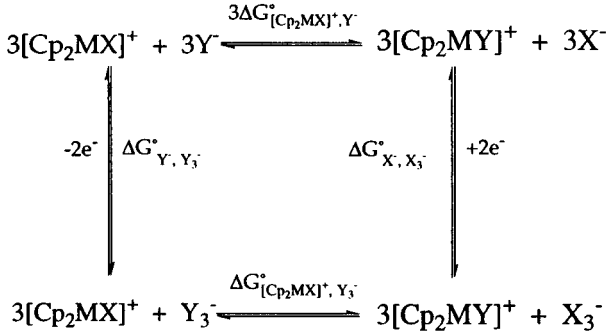

Figure 2. Thermochemical cycle relating reactions 3 and 4.

The relative reactant and transition state energetics, in terms of Figure 1, can be defined by determining the relative reactant state energetics, which, following the approach of Haim,[3] may be obtained from the equilibrium constants for the halide substitution reaction, eq 4. $\Delta G°$ for this reaction represents the

$$[Cp_2MX]^+ + Y^- \rightarrow [Cp_2MY]^+ + X^- \qquad (4)$$

$$\Delta G° = -RT \ln K_{([Cp_2MX]^+,Y^-)}$$

difference in free energy of formation of the solvated $[Cp_2MX]^+$ and $[Cp_2MY]^+$ cations plus the relative free energies of the solvated Y^- and X^- anions. From the known differences in the energies of the solvated halides, the relative reactant state free energies can be obtained from $K_{([Cp_2MX]^+,Y^-)}$.

Direct measurement of these equilibria has proved to be impossible, however. Although the thermodynamic potentials for reduction of $[Cp_2MX]^+$ are not available, it is clear from their chemistry that they are reasonably good oxidants. When halide salts were added to solutions of $[Cp_2MX]^+$, only Cp_2M was observed at equilibrium. The optical spectra of the equilibrium mixtures showed absorptions characteristic of mixed trihalide anions.[23] These results indicate that the net reaction of the halometalloceniums with halide ions is

$$[Cp_2MX]^+ + 2Y^- \rightarrow Cp_2M + [XY_2]^- \qquad (5)$$

It is possible, however, to calculate the equilibrium constants for reaction 4 from the thermochemical cycle given in Figure 2. In the scheme, $\Delta G°_{X^-/X_3}$ represents the standard free energy of the redox reaction $X_3^- + 2e^- \rightarrow 3X^-$. Thermodynamic data for the X^-/X_3^- couples in CH_3CN are available,[24,25] and from the measured standard potentials, the corresponding standard free energy changes can be computed.[26]

The equilibrium constants for reaction 3 for M = Ru, $K_{([Cp_2RuX]^+,Y_3^-)}$, in CD_3CN were determined from the UV−vis and NMR spectra of equilibrium mixtures of haloruthenoceniums with trihalides as described in the Experimental Section. The results are given in Table 2 along with the calculated free energies for direct halide substitution, eq 4. The two electron reduction potentials for $[Cp_2RuX]^+$ have not been measured

(23) Popov, A. I. In *Halogen Chemistry, Vol. 1;* Gutman, V., Ed.; Academic Press: New York, 1967; p 256.
(24) Iwamoto, R. T.; Nelson, I. V. *J. Electroanal. Chem.* **1964**, *7*, 218−221.
(25) (a) Popov, A. I.; Geske, D. H. *J. Am. Chem. Soc.* **1958**, *80*, 1340−1352. (b) Popov, A. I.; Geske, D. H. *J. Am. Chem. Soc.* **1958**, *80*, 5346−5349.
(26) The standard potential ($E°$ vs SCE) and free energy changes ($\Delta G°_{X_3^-,X^-}$) at 298 K in CH_3CN are as follows. Cl:[24] −0.90 V, +170 kJ/mol. Br:[25] −0.53 V, +100 kJ/mol. I:[25] −0.10 V, +20 kJ/mol. The standard deviation of each free energy was estimated to correspond to half of the least significant digit of $E°$ (±0.05 V = ±9.5 kJ/mol).

Table 3. Relative Two Electron Reduction Potentials for $[Cp_2RuX]^+ + 2e^- \rightarrow Cp_2Ru + X^-$ at 298 K in CD_3CN

$[Cp_2RuX]^+$	$E°$ (V vs $E°_{[Cp_2RuCl]^+}$)
$[Cp_2RuCl]^+$	0
$[Cp_2RuBr]^+$	+0.12
$[Cp_2RuI]^+$	+0.25

Table 4. Free Energies[a] of Formation of Solvated X^- at 298 K

	$\Delta G_f°\{X^-(aq)\}$[b]	$\Delta G_{transfer}°\{X^-(aq) \rightarrow X^-(CH_3CN)\}$[c]	$\Delta G_f°\{X^-(CH_3CN)\}$[d]
Cl	−131.25	42.1	−89.2
Br	−103.97	31.3	−72.7
I	−51.59	16.8	−34.8

[a] In kJ/mol. [b] Data from ref 28. [c] Data from ref 29. [d] Estimated error of ±0.06 kJ/mol.

directly by electrochemical methods due to the irreversibility of the couples.[27] The halide substitution equilibrium constants in Table 2 do, however, provide a means of calculating the relative potentials as shown in eq 6.

$$\begin{array}{ll} [Cp_2RuX]^+ + 2e^- \rightarrow Cp_2Ru + X^- & E°_{[Cp_2RuX]^+} \\ Cp_2Ru + Y^- \rightarrow [Cp_2RuY]^+ + 2e^- & -E°_{[Cp_2RuY]^+} \\ \hline [Cp_2RuX]^+ + Y^- \rightarrow [Cp_2RuY]^+ + X^- & E°_{[Cp_2RuX]^+} - E°_{[Cp_2RuY]^+} = \\ & -\Delta G°_{([Cp_2RuX]^+,Y^-)}/nF \end{array} \quad (6)$$

The values of the relative reduction potentials obtained from eq 6 are given in Table 3 and indicate that while the potentials are all very similar, the iodo complex is the most oxidizing and the chloro complex is the least oxidizing. It is not yet possible to directly relate the potentials of the ruthenoceniums to those of the osmoceniums via a common reference couple. It has been previously shown, however, that the haloruthenoceniums will quantitatively oxidize osmocene.[9] Thus, the haloosmoceniums must have reduction potentials at least 120 mV lower than those of the corresponding haloruthenoceniums.

The free energy change for reaction 4 includes the difference in free energies of the solvated halide anions. The free energies of formation of X^- in acetonitrile may be obtained from the free energies of formation of X^-(aq) and the free energies of transfer from water to acetonitrile, given in Table 4. The relative reactant state energies are then given by eq 7. The resulting

$$\Delta\Delta G°_{(X,Y)} = \Delta G_f°\{[Cp_2RuY]^+(solv)\} - \Delta G_f°\{[Cp_2RuX]^+(solv)\} = \Delta G°_{([Cp_2RuX]^+,Y^-)} - [\Delta G_f°\{Y^-(solv)\} - \Delta G_f°\{X^-(solv)\}] \quad (7)$$

differential free energies of formation of the solvated ruthenoceniums, $\Delta\Delta G°_{(X,Y)}$, are given in Table 2. These values represent the differential reactant state energies for the self-exchange reaction as well, since Cp_2Ru(solv) is common to each exchanging couple. The quantitative relative energetics derived from the data in Tables 1 and 2 are illustrated schematically in Figure 3.

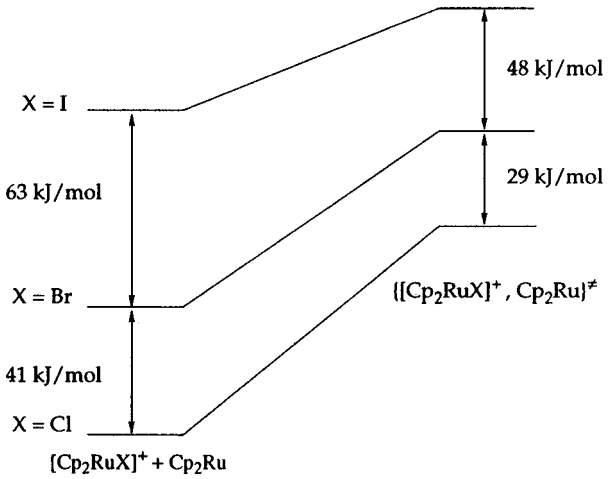

Figure 3. Relative reaction coordinate energetics for the ruthenocenium series at 298 K.

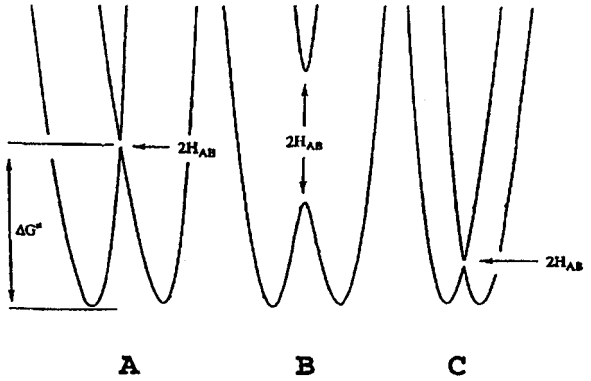

Figure 4. Idealized potential surfaces for coupled multielectron/group transfer: (A) initial energetics; (B) effect of increased electronic coupling; (C) effect of decreased reorganizational energy.

The thermodynamic data in Tables 1 and 2, as illustrated in Figure 3, demonstrate that differences in transition state energies are significantly smaller than the differences in reactant state energies. Such trends in the relative energies have been previously interpreted in terms of net bond breaking in the transition state.[3] In the context of the exchange reactions, contributions to the net bonding character could arise both from weaker $M^{IV}-X$ interactions in the transition state and from differences in desolvation of the transition state based on the identity of X. Such an interpretation would be consistent with the observation that the X = I transfer is more solvent dependent than the X = Br transfer.[10d]

For both ruthenium and osmium, the activation free energies for the self-exchanges vary in the order Cl > Br > I. In terms of general theories of electron or group transfer,[5] there are two contributors to the energies of activation. As illustrated in Figure 4, the energy of activation may be decreased by either increasing the degree of electronic coupling, H_{AB}, between the metal centers in the transition state or decreasing the reorganizational energy required to reach the transition state.

The reorganizational energy associated with the reaction arises from distortion of the system from its equilibrium geometry to that of the transition state. This geometric distortion is related to the differences in the geometries of the oxidized and reduced forms of the species as well as the frequencies of the distorted normal modes. For the group transfer reaction, Cp−M−Cp bending and M−X stretching in the transition state are the principal intramolecular modes along which distortion would be expected to occur. Table 5 summarizes the key parameters for the relevant species which have been structurally character-

(27) McGill, A. D.; Westmoreland, T. D. Unpublished results.
(28) Dascent, W. E. *Inorganic Energetics*; Penguin Books: Victoria, Australia, 1970; pp 132−133.
(29) (a) Marcus, Y. *Pure Appl. Chem.* **1983**, *55*, 977−1021. (b) Sharpe, A. G. *J. Chem. Educ.* **1990**, *67*, 309−315.
(30) Watanabe, M.; Motoyama, I.; Shimoi, M.; Sano, H. *J. Organomet. Chem.* **1996**, *517*, 115−121.
(31) Choi, K. W.; Wan, W. C.; Shea, T. M.; Broderick, W. E.; Westmoreland, T. D. To be published.
(32) Sohn, Y. S.; Schlueter, A. W.; Hendrickson, D. N.; Gray, H. B. *Inorg. Chem.* **1974**, *13*, 301−304.

Table 5. Selected Structural Parameters for $[Cp_2MX]^+$ Salts

salt	ring tilt[a] (deg)	r(M−X) (Å)	ref
$[Cp_2RuCl]BF_4$	34.5	2.417(2)	30
$[Cp_2RuBr]PF_6$	36.7	2.534(2)	31
$[Cp_2RuI]I_3$	32.2	2.732(3)	32
$[Cp_2OsBr]PF_6$	38.2	2.531(2)	31

[a] The angle between the least-squares planes of the carbon atoms of each Cp ring.

ized. From the data in the table, it is apparent that there are only small differences in Cp−M−Cp angles between the metallocenium complexes and that the angles vary in magnitude in the order Br > Cl > I. The vibrational assignments of ruthenocene and osmocene also show that the principal distorting modes have very similar frequencies.[33] Thus, large differences in intramolecular reorganizational energy contributions to the differences in transition state energies can arise only from the asymmetric M−X−M stretch. While detailed assignments have not been made for the metalloceniums, large differences in these frequencies are not expected.[34] While differences in the solvent reorganizational energies also contribute to the differences in activation barriers, the solvent dependencies of several of these reactions[10] indicate that such effects are modest relative to the halide and metal dependencies. Thus, changes in reorganizational energies (Figure 4C) are unlikely to be the source of the strong halide dependence of the rates of self-exchange.

Another major source of the differential energies of activation is the electronic coupling of the metals in the transition state. Figure 5 presents a proposed reaction coordinate and orbital correlation for the coupled two-electron/halide transfer reaction. This proposal seems to be the most reasonable based on the evidence for an inner-sphere mechanism.[35] In the reaction, two electrons in a d_{z^2} orbital of Ru_A^{II} must be transferred to the d_{z^2} orbital of Ru_B^{IV}. As the $[Cp_2Ru^{II}_AX]^+$ ion approaches $Cp_2Ru^{II}_B$ and the $(Ru_A^{IV}-X)-Ru_B^{II}$ interaction begins to occur, the Cp−Ru−Cp angle of $Ru_B^{II}Cp_2$ decreases, leading to the qualitative ordering of the orbitals given in the figure.[36] In the point group

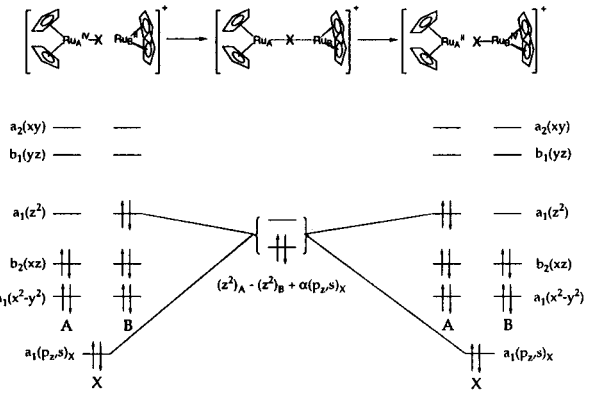

Figure 5. Orbital correlation diagram for $[Cp_2RuX]^+/Cp_2Ru$ exchange based on the proposed linear bridged transition state.

of the transition state, approximately D_{2d}, the orbitals transform as the indicated irreducible representations. The only orbitals on the bridging halide which can mix the d_{z^2} orbitals of the two metals and provide a pathway for electron transfer are those of a_1 symmetry, i.e., the halide valence p_z and s orbitals.

The model in Figure 5 suggests an electronic basis for the strong halide dependence of the exchange rates. For iodide, the p_z orbital is more diffuse than that of chloride, and the overlap with the metal d_{z^2} orbitals is better. Furthermore, the iodide valence orbitals are closer in energy than those of chloride to the metal valence orbitals. These effects lead to stronger mixing of the orbitals and an enhanced electron transfer pathway. The kinetic effects of electronic coupling should be reflected in the $\Delta S^{\ddagger}$ values. The data in Table 1 indicate that the difference in free energies of activation between the bromo- and iodoruthenocenium exchanges lies primarily in the entropic contributions. In this respect, it is curious that the free energies of activation for the corresponding osmocenium exchanges are almost isoentropic. These results suggest that differences in reorganizational energies may be more important for the osmocene series, but the structure of $[Cp_2OsI]^+$ has not yet been reported. Studies to further probe the nature of electronic effects in these complexes are currently underway.

Acknowledgment. The donors of the Petroleum Research Fund, administered by the American Chemical Society, are gratefully acknowledged for support of this work.

Supporting Information Available: Spectroscopic data (NMR, UV−vis) for the complexes, representative EXSY spectrum, tables of 2D integrals and S/N ratios, tabulations and plots of temperature dependent rates, 1D integrals for reaction 3, and fits of UV−vis spectra for reaction 3 (6 pages). Ordering information is given on any current masthead page.

IC961000W

(33) Lokshin, B. V.; Aleksanian, V. T.; Rusach, E. B. *J. Organomet. Chem.* **1975**, *86*, 253−256 and references therein.

(34) The ratio ν_I/ν_{Cl} is typically ∼0.65 for terminal halide complexes and ∼0.5 for bridging halides. This ratio and the relative masses of the halides suggest that the intramolecular reorganization energy for iodide may, in fact, be as much as 1.5 times that for chloride. (a) Clark, R. J. H.; Williams, C. S. *Inorg. Chem.* **1965**, *4*, 350−357. (b) Nakamoto, K. *Infrared and Raman Spectra of Inorganic and Coordination Compounds*, 4th ed; John Wiley and Sons: New York, 1986.

(35) Since there is currently no evidence for a $M^{III}-X-M^{III}$ intermediate, we have assumed that there are no minima along the reaction coordinate other than the reactant and product states. If an intermediate does exist, it is only weakly stabilized relative to the transition state. Further, we cannot at this point completely rule out a metal−metal-bonded dimeric transition state with bridging halide, but this possibility seems unlikely on the basis of steric constraints and the net decrease in bond order in the transition state.

(36) Lauher, J. W.; Hoffman, R. *J. Am. Chem. Soc.* **1976**, *98*, 1729−1742.